Phase Aggregation Suppression of Homogeneous Perovskites Processed in Ambient Condition toward Efficient Light-Emitting Diodes

*Yuqiang Liu, Tongle Bu, Luis K. Ono, Guoqing Tong, Hui Zhang, Yabing Qi**

Energy Materials and Surface Sciences Unit (EMSSU), Okinawa Institute of Science and Technology Graduate University (OIST), 1919-1 Tancha, Onna-son, Kunigami-gun, Okinawa 904-0495, Japan

*Corresponding author: Yabing Qi, Email: Yabing.Qi@OIST.jp

Keywords: perovskites, phase aggregation, antisolvents, energy transfer, light-emitting diodes

Abstract

Perovskite light-emitting diodes (PeLEDs) have attracted attention because of their high efficiencies. However, due to the sensitivity of perovskites to ambient condition, the perovskite emitter layers are generally fabricated under an inert gas environment (e.g., dry N_2), which increases their processing complexity and cost. Here, we report air-prepared quasi-two-dimensional perovskites for efficient PeLEDs. It is found that the phase aggregation is the critical obstacle deteriorating the characteristics of air-prepared perovskites. Through tailoring antisolvent engineering to modulate the nucleation and growth characteristics of perovskite films from precursor solution, phase aggregations are well restrained. Confocal laser scanning fluorescence microscopy results demonstrate homogeneous perovskite films with uniform photoluminescence distributions. Traps at grain boundaries are passivated and excitons transfer among perovskite phases becomes effective. Finally, efficient green PeLEDs based on air-prepared perovskites are realized with an external quantum efficiency of 15.4%. Our work provides a promising strategy to fabricate cost-effective perovskite devices in ambient air condition.

1. Introduction

Metal halide perovskites are emerging as promising semiconductor materials for applications in lighting and display technologies, because of their tunable bandgap, high luminescence efficiency and color purity.[1-3] In recent years, various approaches have been implemented to improve the performance of perovskite light-emitting diodes (PeLEDs).[4-14] Decent efficiencies have been realized with the emission wavelengths ranging from blue, green, red to near-infrared.[15-20] However, perovskite films in these PeLEDs are generally fabricated under a controlled gas atmosphere, mainly due to the strong dependence of the quality of perovskite films on the gas species.[21-22] The controlled atmosphere leads to increased complexity and cost. Therefore, preparing high-quality perovskite films in ambient air would be desirable. To achieve this aim, it is imperative to investigate the influence of preparation conditions of perovskite emitter layers in ambient air on the device performance of PeLEDs.

Among various approaches reported, quasi-two-dimensional (2D) phase perovskites have shown promise for improving the stability of perovskite films against humidity.[23-24] Thus, quasi-2D perovskites may also provide a plausible way to realize air-prepared perovskite emitting layers. A general composition engineering trend to prepare quasi-2D perovskite films is to blend 3D perovskites with hydrophobic bulky organic cations.[23] When these quasi-2D phase perovskites serve as emitter layers, a trend of efficient PeLEDs is reported because of their quantum confinement and morphology control (e.g., small grains, smooth films).[25-28] For instance, Lee and coworkers explored phenylethylammonium (PEA) cations in quasi-2D PeLEDs, and

found that radiative recombination became more effective owing to the exciton confinement and trap passivation, exhibiting a promising alternative to realize efficient PeLEDs.[29] Sargent and coworkers used bulky organic cations to tailor quasi-2D structure perovskites and enhanced dramatically the utilization of charges due to the energy funneling process resulting in an external quantum efficiency (EQE) of 8.8%.[30] Wang and coworkers chose naphthylmethylamine as organic cations to prepare quasi-2D phase perovskites. In this case, an encouraging EQE of 11.7% was reported.[31] Although decent results have been achieved using various quasi-2D perovskites, fabrication of perovskite emitter layers in ambient air has rarely been reported.

The quasi-2D phase PEA-$FAPbBr_3$ (FA=formamidinium) is a representative perovskite for realizing efficient PeLEDs.[32] In this paper, we report the fabrication of efficient PEA-$FAPbBr_3$ based PeLEDs under ambient air condition. Confocal laser scanning fluorescence microscopy (CLSFM) is applied to spatially examine the photoluminescence (PL) emission characteristics of these perovskite films prepared in ambient. We find that the optoelectronic characteristics of perovskite films are sensitive to the type of antisolvent. When chlorobenzene (PhCl) and toluene (PhMe) were used as antisolvents, perovskite films showed inferior PL properties due to poor morphology and phase aggregation. On the other hand, with diethyl ether (DEE) as the antisolvent, we obtained perovskite films with compact morphology and homogeneous phase distribution, which led to reduced leakage current losses and nonradiative recombination pathways. The photoluminescence quantum yield (PLQY) reaches 61.5%. An EQE of 15.4% is obtained in PeLEDs using air-prepared perovskites as

emitter layers.

2. Results and Discussion

Perovskite films are prepared in air with a controlled relative humidity of 15~20% and temperature of 15~20 ℃. Quasi-2D perovskites have been proven to be promising emitters in PeLEDs. Among these quasi-2D perovskites, PEA-$FAPbBr_3$ and PEA-$CsPbBr_3$ are representative and widely used to realize efficient PeLEDs.[32-33] Therefore, PEA-$FAPbBr_3$ and PEA-$CsPbBr_3$ are chosen as the model systems to study perovskite emitters prepared in air condition accordingly. However, as shown in Figure S1a of PEA-$CsPbBr_3$ perovskite films under ultraviolet excitation, air-prepared PEA-$CsPbBr_3$ perovskite films demonstrated non-uniform PL as the growth condition changed from dry N_2 gas to air condition. Hence, quasi-2D PEA-$FAPbBr_3$ perovskite is chosen to study the topic. Quasi-2D phase PEA-$FAPbBr_3$ perovskites are prepared by depositing the perovskite precursor solution containing FABr, $PbBr_2$ and PEABr in dimethyl sulfoxide (DMSO). Three types of solvents, including PhCl (perovskite-PhCl), PhMe (perovskite-PhMe), and DEE (perovskite-DEE), are used as antisolvents to control the growth of perovskites. Figure S1b displays the photographs of perovskite films under 365 nm ultraviolet excitation. The perovskite-DEE film has much stronger PL emission than perovskite-PhCl and perovskite-PhMe films. **Figure 1** shows the CLSFM images of perovskite films. As shown in Figure 1a and b, the perovskite-PhCl films show poor PL characteristics with domain aggregations. The PL intensity in the central area of each perovskite grain is much stronger than that from the boundary region, which

indicates the presence of traps at the grain boundaries.[34] In addition to the poor quality of perovskite grains, the whole perovskite film displays discontinuous morphology. Its corresponding PL intensity distribution (Figure S2a) exhibits a non-uniform status. Similarly, poor PL characteristics are observed in the case of perovskite-PhMe films (Figure 1c, d and Figure S2b). On the other hand, with DEE as the antisolvent, the aggregation is suppressed. The perovskite-DEE film possesses a considerably homogeneous distribution with uniform PL intensity, as evidenced by the CLSFM images (Figure 1e and f) and the corresponding PL intensity distribution (Figure S2c).

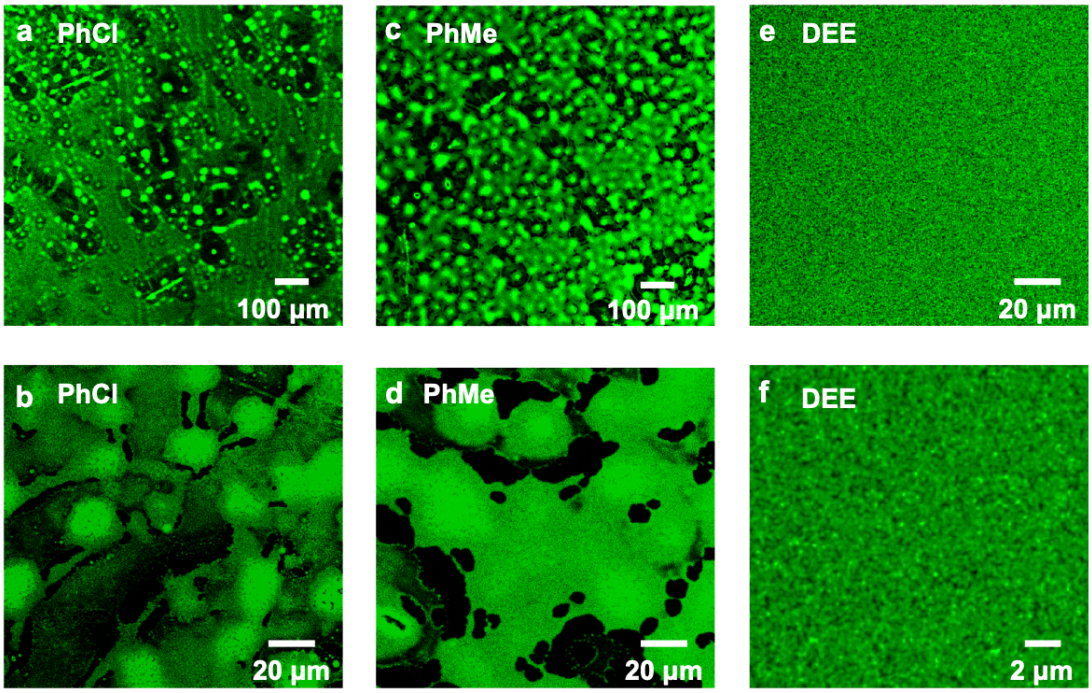

Figure 1. CLSFM mapping images of perovskite films using different antisolvents. a, b) PhCl. c, d) PhMe. e, f) DEE.

Scanning electron microscopy (SEM) measurements were conducted to observe the morphology of perovskite films. The SEM images of the perovskite-PhCl and perovskite-PhMe films in Figure S3a-d clearly show different domains (the dendritic

one of the upper layer and the other one of the lower layer) within the perovskite films, which is detrimental for forming uniform PL distribution. On the contrary, with DEE as the antisolvent (Figure S3e and f), perovskite-DEE films display compact morphology and homogeneous domain distribution. The SEM characteristics correspond well with the PL intensity distribution in Figure 1. Several straight lines are observed on the perovskite films prepared under ambient air condition using DEE as the antisolvent. A plausible reason is the preferential growth of perovskites.[35] Quasi-2D phase structure could serve as a template during the formation of perovskite films, which results in preferred orientation growth of perovskite films. As a consequence, there are several straight lines in perovskite films.

Figure 2a shows the UV-Vis absorption spectra of perovskite films prepared with different antisolvents. The perovskite-DEE film presents a slight blueshift in comparison to the perovskite-PhCl and perovskite-PhMe films. Meanwhile, as shown in the absorption spectra from 425 to 500 nm (Figure S4), both perovskite-PhCl and perovskite-PhMe films have extra excitonic absorption peaks corresponding to quasi-2D perovskites. However, these excitonic peaks do not show in the perovskite-DEE film. According to the steady-state PL spectra in Figure S5, perovskite-PhCl and perovskite-PhMe films show similar 3D perovskite peak positions at 535 nm and 532 nm, respectively. The PL peak blue shifts to 523 nm when using DEE as the antisolvent. The PL intensity of the perovskite-DEE film is much stronger than that of the perovskite-PhCl and perovskite-PhMe films. The stronger PL intensity indicates a more effective radiative recombination.

It is desirable for excitons to transfer from small layer number phases to large layer number phases in quasi-2D perovskites, followed by radiative recombination in these confined 3D perovskites. Under this condition, there is only one steady PL peak.[36] However, as shown in Figure 2b of the steady-state PL spectra on a semi-log scale, when PhCl is used as the antisolvent, there are four PL peaks at 409 nm, 441 nm, 472 nm, and 488 nm corresponding to 1-layer pure-2D, 2-layer, 3-layers, and 4-layer quasi-2D perovskites, respectively. The extra peaks from perovskite-PhCl and perovskite-PhMe films indicate a large number of excitons were captured and recombined at the small layer number pure-2D or quasi-2D phase perovskites during their transfer processes.[28] In the case of perovskite-DEE films, the single PL peak proves more desirable excitons transfer.

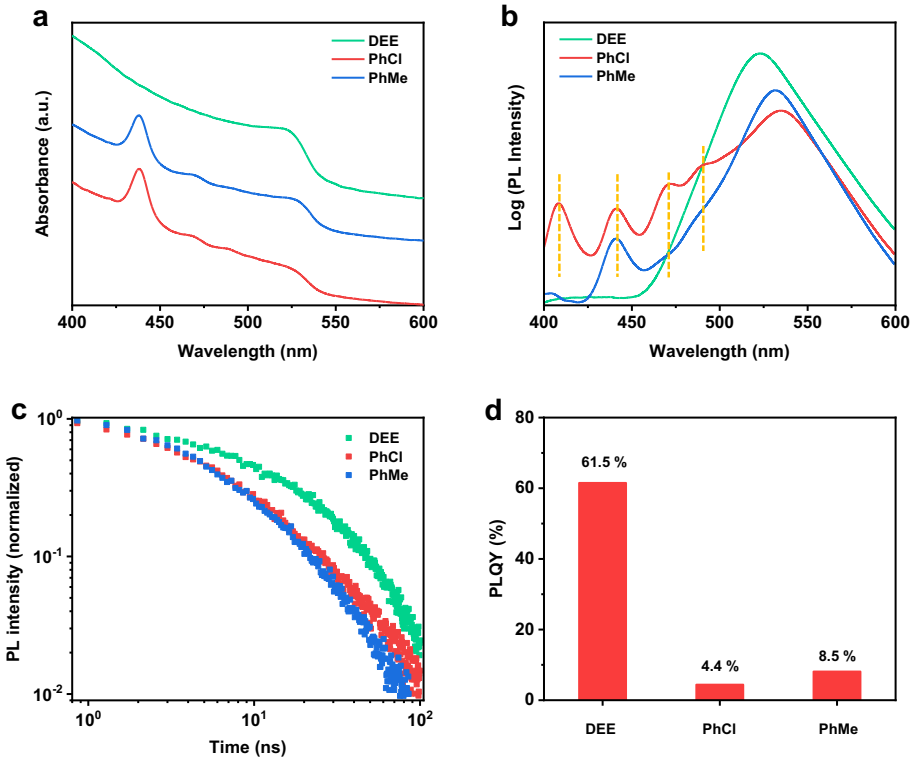

Figure 2. Characteristics of the perovskite films prepared in ambient air with different antisolvents. a) UV-vis absorption spectra. b) Semi-log scale steady-state PL spectra. c)

Time-resolved PL spectra. d) PLQY values.

According to the aforementioned characteristics, perovskite-PhCl and perovskite-PhMe films separate into two different domains (SEM images in Figure S3), and these domains tend to grow individually, leading to uneven PL intensity distribution (CLSFM images in Figure 1a-d). Meanwhile, phase aggregation of low dimensional phase perovskites was observed in perovskite-PhCl or perovskite-PhMe films (absorption spectra and PL spectra in Figure 2a and b). Effective exciton transfer among different perovskite phases is one of the preconditions for realizing high efficiency in quasi-2D PeLEDs.[37] As for the perovskite-PhCl or perovskite-PhMe films, a considerable part of excitons are lost in their transfer pathways, because the severe phase aggregation blocks their transfer. Additionally, the large number of traps around 1 layer pure-2D perovskite surfaces quench charges significantly. On the contrary, the homogeneous phase distribution and uniform morphology of the perovskite-DEE film facilitate the exciton transfer.

The average PL lifetimes (Figure 2c) of the perovskite-PhCl and perovskite-PhMe films are 13.4 ns and 16.6 ns, respectively. The PL lifetime increases to 24.0 ns when DEE is used as the antisolvent. The PL lifetime of the perovskite-DEE film is improved by over 40% than that of the perovskite-PhMe film. The PLQY displays a similar trend, i.e., the PLQY value (Figure 2d) of the perovskite-DEE film (61.5%) is also much higher than that of perovskite-PhCl (4.4%) or perovskite-PhMe (8.1%) films. Two reasons are responsible for the improved PL quality when using the DEE as antisolvent.

The first reason is related to the lower trap concentration at perovskite grain boundaries. The lower trap concentration is favorable to reduce trap-assisted nonradiative recombination losses and utilize charges efficiently.[38-39] The second reason is that the phase aggregation is suppressed. The schematic drawing in **Figure 3** depicts how the phase aggregation causes charge losses. PEA cations result in the formation of quasi-2D phase perovskites with different layer numbers.[29-30] As shown in Figure 3a, excitons can effectively transfer from small layer number phases to large layer number phases, when the quasi-2D phase arrangement is uniform.[33] However, the transfer efficiency can be restricted within aggregated quasi-2D perovskite domains, as shown in Figure 3b. These aggregated domains block and quench charges in the transfer pathways, which enlarges the probability of nonradiative recombination.[37] Meanwhile, part of charges recombines within small layer number phases, resulting in the PL peaks at 409 nm, 441 nm, 472 nm, and 488 nm (Figure 2b). Therefore, the perovskite possesses more effective radiative recombination when DEE is used as the antisolvent.

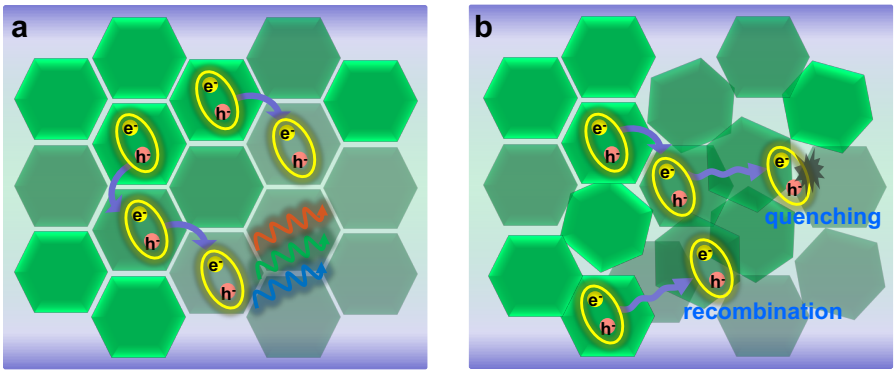

Figure 3. Schematic drawing depicting the influence of phase aggregations. a) Charge transfer processes from small layer number phase to large layer number phase perovskites. b) Charge recombination or quenching during their transfer processes

caused by phase aggregations.

To understand the perovskite growth mechanism with different antisolvents, the phase formation of perovskites was explored without as well as with different antisolvents. **Figure 4**a shows the semi-log scale XRD patterns of fresh perovskite before the annealing process. The fresh perovskite film without antisolvents (reference) showed strong 2-layered quasi-2D phase diffraction peaks at 4.0° and 7.9°. The strong intensity peaks at 5.3° and 10.6° belong to the 1-layered pure-2D phase. The diffraction peak at 14.8° corresponds to the 3D phase perovskite. The corresponding SEM image (Figure 4b, reference) shows a typical quasi-2D perovskite morphology with unclear grain boundaries and needle-like 3D crystals.[40-41] It indicates phase segregation into quasi-2D and 3D domains in the perovskite films without antisolvents. After the antisolvent process, the diffraction peaks of both quasi-2D and 3D perovskites decrease markedly as shown in Figure S6. Especially, the perovskite-DEE film possesses fewer quasi-2D diffraction peaks than other films (Figure 4a). On the other hand, two different types of domains appear in fresh perovskite-PhCl and perovskite-PhMe films as shown in the SEM images (Figure 4b, PhCl and PhMe). Meanwhile, each of the domains tends to be aggregated leading to heterogeneous perovskite films, instead of mixing uniformly. But the DEE processed fresh film still maintains a homogenous morphology with small grain sizes (Figure 4b, DEE).

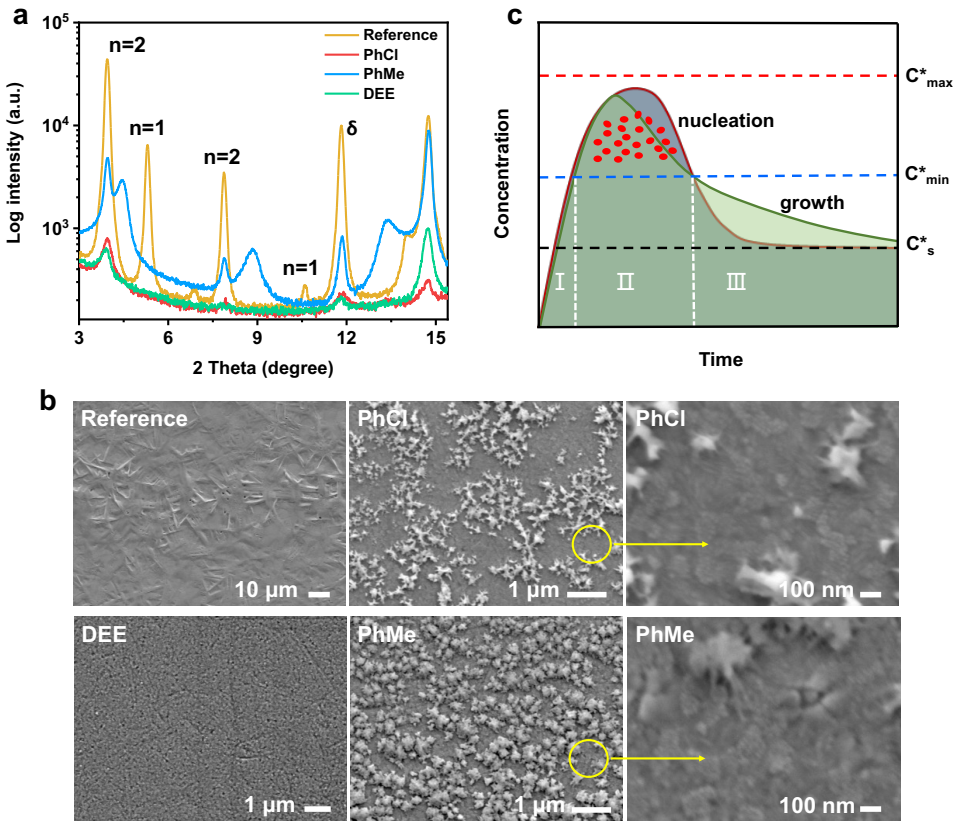

Figure 4. Characteristics of the perovskite films before annealing processes. a) XRD patterns of the fresh perovskite films. b) SEM images of the perovskite films prior to annealing. c) LaMer diagram of nucleation and growth of perovskites.

Furthermore, we dropped different antisolvents into the perovskite precursor solution respectively to explore the difference induced by these different antisolvents. As shown in Figure S7, when DEE was dropped into the precursor, the solution turned into a layered structure quickly. However, after dropping PhCl or PhMe, the solution became turbid and after several seconds became layered. In other words, the extraction rate of DEE to DMSO is much faster than that of PhCl or PhMe. The nucleation and growth dynamics in these cases can be depicted by the Lamer curve as shown in Figure 4c.[42] In general, there are three portions in the LaMer diagram: (i) monomers

accumulation in the solution, (ii) nucleation burst once the monomer concentration over the minimum supersaturation limit, and (iii) subsequent nuclei growth controlled by growing species diffusion. Based on the LaMer mechanism, the faster volatilization of host solvents contributes to the faster nucleation of perovskites, and thus more homogeneous films can be obtained.[43] The DEE antisolvent is favorable to remove the DMSO quickly, which increases the supersaturation instantaneously and produces plenty of smaller nuclei, suppresses the growth of quasi-2D perovskite phases, and thus contributes to homogenous morphology. In this case, the disturbance of ambient water to perovskite growth is also eliminated effectively. The weak extraction ability of PhCl and PhMe solvents leads to a large number of DMSO-contained intermediate phases. These phases cannot be successfully converted into perovskite grains uniformly due to the disturbance of ambient water.[21] The fast growth of quasi-2D phases further causes poor morphology with obvious phase aggregation in perovskite-PhCl and perovskite-PhMe films. These morphologies are almost unchanged even after thermal annealing processes (Figure S3).

The PeLED devices are fabricated on indium tin oxide (ITO) glass substrates with a structure of ITO/poly(3,4-ethylenedioxythiophene): poly(styrenesulfonate) (PEDOT: PSS)/perovskites/2,2',2''-(1,3,5-benzenetriyl) tris-(1-phenyl-1Hbenzimidazole) (TPBi)/8-hydroxyquinolinolato-lithium (Liq)/aluminum (Al). The conduction band and valence band (**Figure 5**a) of perovskite films are calculated based on the ultraviolet photoemission spectroscopy (UPS) results (Figure S8) and the bandgap information determined by UV-vis absorption experiments (Figure 2a). Because of the poor quality

of perovskite-PhCl and perovskite-PhMe films, injected charges lose through leakage current and traps quenching. Hence, the corresponding PeLEDs display inferior diode characteristics without electroluminescence (EL) emission, as shown in Figure S9 of the current density-voltage curves. The better electrical properties of devices are obtained in the case of perovskite-DEE films. Figure 5b is the EL spectra of devices under different voltages. The EL peaks are located at 525 nm with a Commission Internationale de l'Eclairage (CIE) color coordinate of (0.16, 0.77) in Figure S10. Meanwhile, there is no obvious shift of EL peaks with increasing the applied voltages. The turn-on voltage of devices is 3 V, according to the current density-luminance-voltage curves in Figure 5c. The highest luminance reaches 11765 cd/m^2 at the applied voltage of 6.0 V. The EQE curve is presented in Figure 5d. The maximum EQE reaches 15.4% that is comparable with the previous PeLEDs fabricated in a controlled nitrogen atmosphere.[32] Figure S11 is the corresponding EQE-brightness curve of devices. The operational stability is also measured, as shown in Figure S12. When the initial luminance is 100 cd/m^2, the half-lifetime of devices reaches 19 minutes.

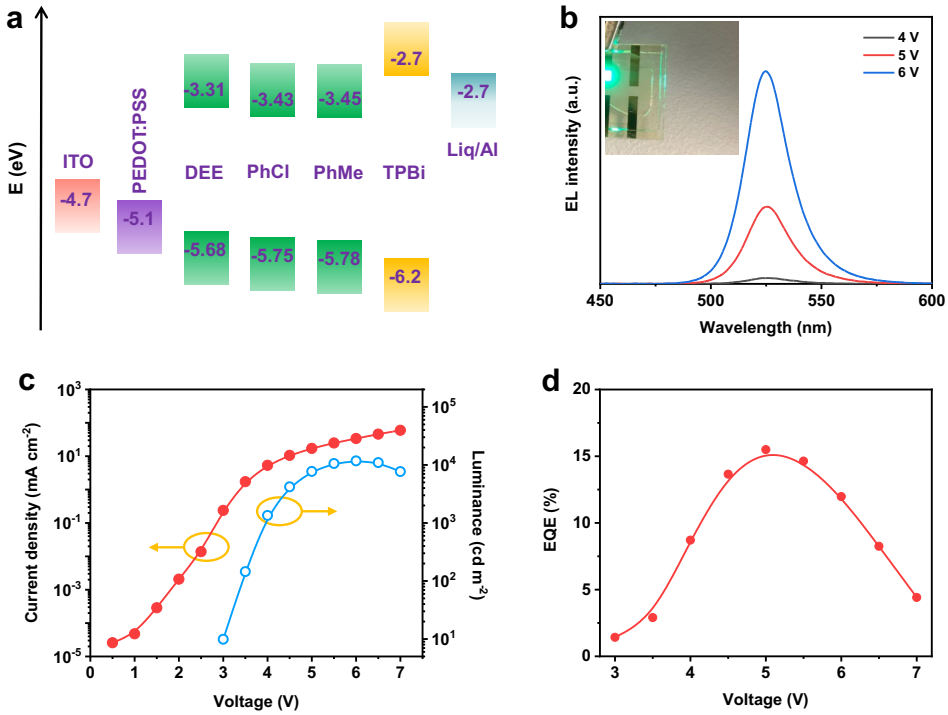

Figure 5. Optoelectronic performance characterization. a) Band energy diagram of PeLEDs with different perovskite emitter layers. b) EL spectra of PeLEDs with DEE as the antisolvent. The photograph is a device under 5 V bias. c) Current density-luminance-voltage curves and d) EQE-voltage curves of PeLEDs with DEE as the antisolvent.

3. Conclusion

In summary, we report air-prepared quasi-2D perovskite films with good optoelectronic properties, through controlling the nucleation and growth processes of perovskite films by antisolvent engineering. The phase distribution is of importance to the properties of perovskite films. Homogeneous phase distributions are realized in perovskites when a suitable antisolvent is used. Excitons transfer becomes effective and nonradiative recombination losses are suppressed. Consequently, efficient green PeLEDs with an

EQE of 15.4% are achieved with the air-prepared perovskite films as emitter layers.

Supporting Information

Supporting Information is available from the Wiley Online Library or from the author.

Acknowledgements

This work was supported by funding from the Energy Materials and Surface Sciences Unit of the Okinawa Institute of Science and Technology Graduate University, the OIST R&D Cluster Research Program, the OIST Proof of Concept (POC) Program, and JST A-STEP Grant Number JPMJTM20HS, Japan. We thank the OIST Micro/Nanofabrication Section and Imaging Section for the support.

Conflict of Interest

The authors declare no conflict of interest.

References

[1] X. K. Liu, W. Xu, S. Bai, Y. Jin, J. Wang, R. H. Friend, F. Gao, *Nat. Mater.* **2021**, *20*, 10.

[2] M. H. Park, J. S. Kim, J. M. Heo, S. Ahn, S. H. Jeong, T. W. Lee, *ACS Energy Lett.* **2019**, *4*, 1134.

[3] L. N. Quan, B. P. Rand, R. H. Friend, S. G. Mhaisalkar, T. W. Lee, E. H. Sargent, *Chem. Rev.* **2019**, *119*, 7444.

[4] Z. K. Tan, R. S. Moghaddam, M. L. Lai, P. Docampo, R. Higler, F. Deschler, M. Price, A. Sadhanala, L. M. Pazos, D. Credgington, F. Hanusch, T. Bein, H. J. Snaith, R. H. Friend, *Nat. Nanotechnol.* **2014**, *9*, 687.

[5] J. Song, J. Li, X. Li, L. Xu, Y. Dong, H. Zeng, *Adv. Mater.* **2015**, *27*, 7162.

[6] H. Cho, S. H. Jeong, M. H. Park, Y. H. Kim, C. Wolf, C. L. Lee, J. H. Heo, A. Sadhanala, N. Myoung, S. Yoo, S. H. Im, R. H. Friend, T. W. Lee, *Science* **2015**, *350*, 1222.

[7] Z. Xiao, R. A. Kerner, L. Zhao, N. L. Tran, K. M. Lee, T.-W. Koh, G. D. Scholes, B. P. Rand, *Nat. Photonics* **2017**, *11*, 108.

[8] Y. Shen, L. P. Cheng, Y. Q. Li, W. Li, J. D. Chen, S. T. Lee, J. X. Tang, *Adv. Mater.* **2019**, *31*, 1901517.

[9] Y. Guo, Y. Jia, N. Li, M. Chen, S. Hu, C. Liu, N. Zhao, *Adv. Funct. Mater.* **2020**, *30*, 1910464.

[10] H. C. Wang, W. Wang, A. C. Tang, H. Y. Tsai, Z. Bao, T. Ihara, N. Yarita, H. Tahara, Y. Kanemitsu, S. Chen, R. S. Liu, *Angew. Chem. Int. Ed.* **2017**, *56*, 13650.

[11] M. R. Leyden, L. Meng, Y. Jiang, L. K. Ono, L. Qiu, E. J. Juarez-Perez, C. Qin, C. Adachi, Y. B. Qi, *J. Phys. Chem. Lett.* **2017**, *8*, 3193.

[12] W.-C. Lai, W.-M. Hsieh, S.-H. Yang, J.-C. Yang, T.-F. Guo, P. Chen, L.-J. Lin, H.-C. Hsu, *ACS Omega* **2020**, *5*, 8697.

[13] J. N. Yang, Y. Song, J. S. Yao, K. H. Wang, J. J. Wang, B. S. Zhu, M. M. Yao, S. U. Rahman, Y. F. Lan, F. J. Fan, H. B. Yao, *J. Am. Chem. Soc.* **2020**, *142*, 2956.

[14] Y. Liu, L. K. Ono, G. Tong, H. Zhang, Y. B. Qi, *ACS Energy Lett.* **2021**, *6*, 908.

[15] Z. Chu, Y. Zhao, F. Ma, C.-X. Zhang, H. Deng, F. Gao, Q. Ye, J. Meng, Z. Yin, X. Zhang, J. You, *Nat. Commun.* **2020**, *11*, 4165.

[16] T. Chiba, Y. Hayashi, H. Ebe, K. Hoshi, J. Sato, S. Sato, Y. J. Pu, S. Ohisa, J. Kido, *Nat. Photonics* **2018**, *12*, 681.

[17] Y. Dong, Y. K. Wang, F. Yuan, A. Johnston, Y. Liu, D. Ma, M. J. Choi, B. Chen, M. Chekini, S. W. Baek, L. K. Sagar, J. Fan, Y. Hou, M. Wu, S. Lee, B. Sun, S. Hoogland, R. Quintero-Bermudez, H. Ebe, P. Todorovic, F. Dinic, P. Li, H. T. Kung, M. I. Saidaminov, E. Kumacheva, E. Spiecker, L. S. Liao, O. Voznyy, Z. H. Lu, E. H. Sargent, *Nat. Nanotechnol.* **2020**, *15*, 668.

[18] M. Karlsson, Z. Yi, S. Reichert, X. Luo, W. Lin, Z. Zhang, C. Bao, R. Zhang, S. Bai, G. Zheng, P. Teng, L. Duan, Y. Lu, K. Zheng, T. Pullerits, C. Deibel, W. Xu, R. Friend, F. Gao, *Nat. Commun.* **2021**, *12*, 361.

[19] W. D. Xu, Q. Hu, S. Bai, C. X. Bao, Y. F. Miao, Z. C. Yuan, T. Borzda, A. J. Barker, E. Tyukalova, Z. J. Hu, M. Kawecki, H. Y. Wang, Z. B. Yan, X. J. Liu, X. B. Shi, K. Uvdal, M. Fahlman, W. J. Zhang, M. Duchamp, J. M. Liu, A. Petrozza, J. P. Wang, L. M. Liu, W. Huang, F. Gao, *Nat. Photonics* **2019**, *13*, 418.

[20] C. Kuang, Z. Hu, Z. Yuan, K. Wen, J. Qing, L. Kobera, S. Abbrent, J. Brus, C. Yin, H. Wang, W. Xu, J. Wang, S. Bai, F. Gao, *Joule* **2021**, *5*, 618.

[21] K. Zhang, Z. Wang, G. Wang, J. Wang, Y. Li, W. Qian, S. Zheng, S. Xiao, S. Yang, *Nat. Commun.* **2020**, *11*, 1006.

[22] H.-S. Ko, J.-W. Lee, N.-G. Park, *J. Mater. Chem. A* **2015**, *3*, 8808.

[23] F. Zhang, H. Lu, J. Tong, J. J. Berry, M. C. Beard, K. Zhu, *Energy Environ. Sci.* **2020**, *13*, 1154.

[24] L. K. Ono, Y. B. Qi, S. F. Liu, *Joule* **2018**, *2*, 1961.

[25] L. Cheng, T. Jiang, Y. Cao, C. Yi, N. Wang, W. Huang, J. Wang, *Adv. Mater.* **2019**, *32*, 1904163.

[26] Y. Liu, L. K. Ono, Y. B. Qi, *InfoMat.* **2020**, *2*, 1095.

[27] J. Si, Y. Liu, Z. He, H. Du, K. Du, D. Chen, J. Li, M. Xu, H. Tian, H. He, D. Di, C. Lin, Y. Cheng, J. Wang, Y. Jin, *ACS Nano* **2017**, *11*, 11100.

[28] Y. Liu, J. Y. Cui, K. Du, H. Tian, Z. F. He, Q. H. Zhou, Z. L. Yang, Y. Z. Deng, D. Chen, X. B. Zuo, Y. Ren, L. Wang, H. M. Zhu, B. D. Zhao, D. W. Di, J. P. Wang, R. H. Friend, Y. Z. Jin, *Nat. Photonics* **2019**, *13*, 760.

[29] J. Byun, H. Cho, C. Wolf, M. Jang, A. Sadhanala, R. H. Friend, H. Yang, T. W. Lee, *Adv. Mater.* **2016**, *28*, 7515.

[30] M. Yuan, L. N. Quan, R. Comin, G. Walters, R. Sabatini, O. Voznyy, S. Hoogland, Y. Zhao, E. M. Beauregard, P. Kanjanaboos, Z. Lu, D. H. Kim, E. H. Sargent, *Nat. Nanotechnol.* **2016**, *11*, 872.

[31] N. Wang, L. Cheng, R. Ge, S. Zhang, Y. Miao, W. Zou, C. Yi, Y. Sun, Y. Cao, R. Yang, Y. Wei, Q. Guo, Y. Ke, M. Yu, Y. Jin, Y. Liu, Q. Ding, D. Di, L. Yang, G. Xing, H. Tian, C. Jin, F. Gao, R. H. Friend, J. Wang, W. Huang, *Nat. Photonics* **2016**, *10*, 699.

[32] X. Yang, X. Zhang, J. Deng, Z. Chu, Q. Jiang, J. Meng, P. Wang, L. Zhang, Z.

Yin, J. You, *Nat. Commun.* **2018**, *9*, 570.

[33] M. Ban, Y. Zou, J. P. H. Rivett, Y. Yang, T. H. Thomas, Y. Tan, T. Song, X. Gao, D. Credington, F. Deschler, H. Sirringhaus, B. Sun, *Nat. Commun.* **2018**, *9*, 3892.

[34] F. Li, X. Deng, F. Qi, Z. Li, D. Liu, D. Shen, M. Qin, S. Wu, F. Lin, S. H. Jang, J. Zhang, X. Lu, D. Lei, C. S. Lee, Z. Zhu, A. K. Jen, *J. Am. Chem. Soc.* **2020**, *142*, 20134.

[35] G. Tong, M. Jiang, D.-Y. Son, L. Qiu, Z. Liu, L. K. Ono, Y. Qi, *ACS Appl. Mater. Interfaces* **2020**, *12*, 14185.

[36] Z. Ren, J. Yu, Z. Qin, J. Wang, J. Sun, C. C. S. Chan, S. Ding, K. Wang, R. Chen, K. S. Wong, X. Lu, W. J. Yin, W. C. H. Choy, *Adv. Mater.* **2021**, *33*, 2005570.

[37] B. D. Zhao, S. Bai, V. Kim, R. Lamboll, R. Shivanna, F. Auras, J. M. Richter, L. Yang, L. J. Dai, M. Alsari, X. J. She, L. S. Liang, J. B. Zhang, S. Lilliu, P. Gao, H. J. Snaith, J. P. Wang, N. C. Greenham, R. H. Friend, D. W. Di, *Nat. Photonics* **2018**, *12*, 783.

[38] Y. Liu, L. Cai, Y. Xu, J. Li, Y. Qin, T. Song, L. Wang, Y. Li, L. K. Ono, Y. B. Qi, B. Sun, *Nano Energy* **2020**, *78*, 105134.

[39] J. W. Lee, Y. J. Choi, J. M. Yang, S. Ham, S. K. Jeon, J. Y. Lee, Y. H. Song, E. K. Ji, D. H. Yoon, S. Seo, H. Shin, G. S. Han, H. S. Jung, D. Kim, N. G. Park, *ACS Nano* **2017**, *11*, 3311.

[40] F. Huang, Y. Dkhissi, W. Huang, M. Xiao, I. Benesperi, S. Rubanov, Y. Zhu, X. Lin, L. Jiang, Y. Zhou, A. Gray-Weale, J. Etheridge, C. R. McNeill, R. A. Caruso, U. Bach, L. Spiccia, Y.-B. Cheng, *Nano Energy* **2014**, *10*, 10.

[41] C. Zuo, L. Ding, *Angew. Chem. Int. Ed.* **2021**, *60*, 11242.

[42] C. Liu, Y. B. Cheng, Z. Ge, *Chem. Soc. Rev.* **2020**, *49*, 1653.

[43] F. Huang, A. R. Pascoe, W. Q. Wu, Z. Ku, Y. Peng, J. Zhong, R. A. Caruso, Y. B. Cheng, *Adv. Mater.* **2017**, *29*, 1601715.

Table of Contents

Air-prepared homogeneous quasi-two-dimensional perovskites are formed through suppressing the adverse phase aggregation. Excitons transfer among different perovskite phases becomes effective and an external quantum efficiency of 15.4% is realized in green perovskite light-emitting diodes.

Yuqiang Liu, Tongle Bu, Luis K. Ono, Guoqing Tong, Hui Zhang, Yabing Qi*

Phase Aggregation Suppression of Homogeneous Perovskites Processed in Ambient Condition toward Efficient Light-Emitting Diodes